

## 4f excitation energies in rare-earth metals: Relativistic calculations

J. F. Herbst\*†‡

National Bureau of Standards, Washington, D. C. 20234

R. E. Watson

Brookhaven National Laboratory, § Upton, New York 11973

J. W. Wilkins†

Laboratory of Atomic and Solid State Physics, Materials Science Center, Cornell University, Ithaca, New York 14853

(Received 22 October 1975)

We describe calculations of 4f electron binding energies for the rare-earth metals. Relativistic Hartree-Fock calculations for atomic configurations most closely approximating those of the metals are initially performed, and crystal potentials are constructed by means of the renormalized-atom method. Relativistic band calculations are iterated to crude self-consistency and total band energies obtained. Correlation effects identical to those in the free atoms are assumed. Within the assumption of a completely screened final state, in which the atomic site having the 4f hole is electrically neutral, 4f binding energies are estimated which are in at least as good agreement with experiment as previous, less complete calculations. The impact of the complete screening approximation is assessed by estimating the binding energies corresponding to atomic sites which are ionized in their final states; we find that the presence of an additional screening electron lowers the 4f binding energy by 4–6 eV.

### I. INTRODUCTION

In a previous publication<sup>1</sup> (hereafter referred to as I) calculations of 4f electron excitation energies in the rare-earth metals were reported. The computations were performed within the framework of the renormalized-atom method and relied upon *nonrelativistic* Hartree-Fock (NRHF) free-atom solutions. Also, the energy-band results describing the metals were not self-consistent, i. e., the crystal potentials were not constructed with wave functions consistent with the potentials from which they were computed. Here we present results for 4f excitation energies calculated once more in the spirit of the renormalized-atom method but employing *relativistic* Hartree-Fock (RHF) atomic solutions as well as the imposition of crude self-consistency in band potential construction.

As in I, we find that the 4f one-electron energies grossly overestimate the observed binding energies and, following I, we estimate the total energy difference

$$\Delta_-(f^n \rightarrow f^{n-1}) \equiv E_{\text{metal}} [4f^{n-1}(5d6s)^{m'}] - E_{\text{metal}} [4f^n(5d6s)^m], \quad (1)$$

where the  $E$ 's are total energies per cell of the metal. Provided correlation effects are taken into account, this provides an excellent description of 4f binding energies in the metals. We use Hartree-Fock (HF) calculations for the free atom and the metal to estimate the difference in 4f excitation energy between the free atom and metal; to this is added the experimentally determined free-atom excitation energy:

$$\Delta_-(f^n \rightarrow f^{n-1}) = \{E_{\text{metal}}^{\text{HF}} [4f^{n-1}(5d6s)^{m'}] - E_{\text{metal}}^{\text{HF}} [4d^n(5d6s)^m]\} - \{E_{\text{atom}}^{\text{HF}} [4f^{n-1}5d^{m'-1}6s] - E_{\text{atom}}^{\text{HF}} [4f^n5d^{m-1}6s]\} + \{E_{\text{atom}} [4f^{n-1}5d^{m'-1}6s] - E_{\text{atom}} [4f^n5d^{m-1}6s]\}_{\text{expt}} \equiv E_{\text{metal}}^{\text{HF}} [4f^{n-1}(5d6s)^{m'}] E_{\text{metal}}^{\text{HF}} [4f^n(5d6s)^m] + \xi. \quad (2)$$

NRHF calculations were employed in I, and the resulting free-atom correlation energy difference  $\xi$  incorporated both correlation and relativistic contributions; RHF calculations are employed here, and  $\xi$  contains only correlation terms. The trend in the  $\xi$  we obtain in this work agrees well with intuitive expectations of correlation effects associated with 4f excitation. The assumption of common 4f correlation effects in the free atom and in the metal is plausible and is apparently borne

out by the agreement of our calculated  $\Delta_-$  values with experiment.

One of the principal assumptions of I was the "complete screening" approximation employed in calculating the energy of a cell in the metal excited by photoejection of a 4f electron; charge neutrality was maintained by describing the excited cell with a band structure appropriate to a configuration having one fewer 4f and one more conduction electron, i. e.,  $m' = m + 1$  in Eqs. (1) and (2).

Section II describes relativistic, self-consistent calculations done in this approximation. In Sec. III we examine the "unscreened" limit in which the atomic cell has a charge of  $+1|e|$  after photoexcitation:  $m'=m$ . This procedure overestimates the  $4f$  binding energy and, in fact, suggests that the  $4f$  photoemission event corresponds closely to the complete screening limit.

## II. $\Delta$ CALCULATIONS: COMPLETE SCREENING APPROXIMATION

We describe in this section our calculations of  $\Delta$ , incorporating both relativistic atomic solutions and specific band self-consistency criteria; the complete screening approximation is invoked, and so the results represent the relativistic, self-consistent analog of those presented in I. As has already been noted, band calculations are done for the metal in its final as well as initial state. The problem of a single  $4f^{n-1}$  impurity embedded in a  $4f^n$  host is replaced by the question of estimating the energy required to change the valence of the entire metal. This is a much more tractable problem.

The renormalized-atom method<sup>2</sup> forms the basis of our approach. The atomic configuration  $4f^n 5d^{m-1} 6s$  is assumed appropriate to the metal;  $m$ , the valence, is equal to three for all the rare-earth metals with the exception of europium and ytterbium, for which  $m=2$ . RHF free-atom solutions are obtained for the configuration of interest through the use of Lindgren's average of  $LS$  configuration scheme<sup>3</sup> which involves averaging over the  $L$ ,  $S$ ,  $M_L$ , and  $M_S$  quantum numbers of the open shells. The free-atom wave functions are truncated at  $r_{WS}$ , the Wigner-Seitz radius of the metal, and normalized to unity within the Wigner-Seitz sphere; initial band potentials are then constructed with the truncated wave functions.  $5d$  and  $6s$  band extrema are determined by imposing Wigner-Seitz-type<sup>1,2</sup> boundary conditions at  $r_{WS}$  on the large components of the wave functions obtained from integration of the Dirac-Fock equations.<sup>3,4</sup> That is, the potential (for either a  $5d$  or  $6s$  electron) is used in the Dirac-Fock equations, which are integrated to yield wave functions over a range of energies  $\epsilon$ . The value of  $\epsilon$  for which the large component of the wave function has zero derivative at  $r_{WS}$  specifies the bottom of the appropriate band; the  $\epsilon$  for which the large component of the  $5d$  wave function is zero at  $r_{WS}$  determines the top of the  $d$ -band.<sup>5</sup> These criteria were found<sup>2</sup> to determine band extrema to  $\sim 0.1$  eV.

### A. Band self-consistency

Permitting the  $5d$  and  $6s$  occupancies to be non-integral, the band calculations are iterated to crude self-consistency in the following way. The

Fermi level  $\epsilon_F$  is determined by assuming a parabolic  $s$ -band and a rectangular  $d$ -band density of states; admittedly this is a great oversimplification, but it suffices for the almost unfilled  $d$  bands of concern to us here. Wave functions for the  $5d$  and  $6s$  electrons are found at average energies in the occupied bands;  $5d$  and  $6s$  contributions to the band potentials are estimated by reconstructing the potentials with these average wave functions. Band extrema are again determined and the procedure repeated until  $\epsilon_{r_1}$  and the  $d$ -band extrema have converged to within 0.005 eV. The total Hartree-Fock band energy  $E_{\text{band}}^{\text{RHF}}$  and one-electron energies  $\epsilon_i$  are then evaluated. These quantities are given by the standard expressions<sup>4</sup> but are computed with the renormalized wave functions, including the self-consistent average  $5d$  and  $6s$  wave functions and occupation numbers. We emphasize that  $E_{\text{band}}^{\text{RHF}}$  is the total RHF energy of *all* the electrons in a Wigner-Seitz sphere of the metal. We expect an uncertainty of less than 0.3 eV in  $E_{\text{band}}^{\text{RHF}}$  and less than 0.5 eV in  $\epsilon_F - \epsilon_{4f}$ , the  $4f$  one-electron energy measured with respect to the Fermi level.

### B. Correlation and Hund's rules

Lacking a method of calculating the correlation energy in the metallic state, we make use of the free-atom correlation energy difference between the two free-atom configurations connected with the  $\Delta$  estimate. Except for Eu and Yb, however, the transition of interest is  $f^n d^2 s \rightarrow f^{n-1} d^3 s$ , for which no reliable atomic spectral information exists. We are consequently compelled to use the spectral data available for the  $f^n ds \rightarrow f^{n-1} d^2 s$  transition, involving the same number of  $4f$  electrons but corresponding to the preceding element in the periodic table. The free-atom correlation energy difference  $\xi$  for this transition is defined as

$$\begin{aligned} \xi &\equiv E_{\text{corr}}(f^{n-1} d^2 s) - E_{\text{corr}}(f^n ds) = [E(f^{n-1} d^2 s)_{\text{expt}} \\ &\quad - E_{\text{gnd}}^{\text{RHF}}(f^{n-1} d^2 s)] - [E(f^n ds)_{\text{expt}} - E_{\text{gnd}}^{\text{RHF}}(f^n ds)] \\ &= [E(f^{n-1} d^2 s) - E(f^n ds)]_{\text{expt}} \\ &\quad - [E_{\text{gnd}}^{\text{RHF}}(f^{n-1} d^2 s) - E_{\text{gnd}}^{\text{RHF}}(f^n ds)]. \end{aligned} \quad (3)$$

The first bracket in the last line of Eq. (3) is supplied by experimental spectral data,<sup>6</sup> while the second bracket is based on our RHF calculations for the same atom. The calculations involve the average of  $LS$  configuration scheme, and we correct the total energy to correspond to the proper atomic ground state through the use of multiplet theory and denote that energy by  $E_{\text{gnd}}^{\text{RHF}}$ ; the correction is described in the Appendix. The value of  $\xi$  for the  $f^8 d^2 s - f^7 d^3 s$  transition appropriate to the Tb  $\Delta$  estimate, for example, is thus taken to be that for the  $f^8 ds - f^7 d^2 s$  transition in Gd.

This drastic but inescapable assumption is employed in all the  $\Delta_-$  estimates for the trivalent metals; for divalent Eu and Yb the corresponding free-atom transition is of the form  $f^n ds \rightarrow f^{n-1} d^2 s$ , for which atomic spectral information on which to base  $\xi$  exists.

In the initial state the 4f electrons, to very good approximation, are in the Hund's-rule ground

$$\Delta_- = \xi + [E(f^{n-1} d^m s) - E(f^n d^{m-1} s)]_{(LS \text{ av})}^{\text{RHF}} + [E(f^{n-1}) - E(f^n)]_{4f \text{ Hund's-rule correction}} + \{[E_{\text{band}}^{\text{RHF}}(f^{n-1}(ds)^{m+1}) - E_{(LS \text{ av})}^{\text{RHF}}(f^{n-1} d^m s)] - [E_{\text{band}}^{\text{RHF}}(f^n(ds)^m) - E_{(LS \text{ av})}^{\text{RHF}}(f^n d^{m-1} s)]\} \equiv \xi + \delta E(\text{atom}) + \delta E(\text{Hund}) + \delta E(\text{atom} \rightarrow \text{band}).$$

(4)

$\xi$  is defined by Eq. (3), the first term in brackets [ $\delta E(\text{atom})$ ] is the difference between the initial- and final-state total energies from our average of  $LS$  configuration atomic calculations, the second bracketed term [ $\delta E(\text{Hund})$ ] is the correction due to placing the 4f electrons in the proper initial- and final-state Hund's rule multiplets; and the last term [ $\delta E(\text{atom} \rightarrow \text{band})$ ] is the free-atom  $\rightarrow$  metal difference in excitation energy which employs our self-consistent band calculations for the 5d and 6s electrons. These components of  $\Delta_-$  are given in Table I. It is clear that the correlation energy difference  $\xi$  is substantial and its sign indicates that correlation effects are more important in a configuration with one more 4f and one fewer 5d electron, which is not surprising. Specifically, we see this by rewriting Eq. (3)

$$\xi = [E_{\text{nd}}^{\text{RHF}}(f^n ds) - E(f^n ds)_{\text{expt}}] - [E_{\text{nd}}^{\text{RHF}}(f^{n-1} d^2 s) - E(f^{n-1} d^2 s)_{\text{expt}}]. \quad (5)$$

There is a general increase in  $\xi$  across the row; when the number of  $f$  electrons  $n$  is less than or equal to 7 all the  $f$  spins are parallel, but for  $n > 7$  there are 7 majority and  $n - 7$  minority spins, and correlation effects are more substantial.

From Table I we see that the sum  $\xi + \delta E(\text{atom} \rightarrow \text{band})$  displays a much smaller variation across the row than does  $\delta E(\text{atom}) + \delta E(\text{Hund})$ . In fact, the experimental trend in  $\Delta_-$  is roughly reproduced by neglecting  $\xi$  and  $\delta E(\text{atom} \rightarrow \text{band})$  and employing the atomic HF terms alone. Both correlation and band effects are important, and the extent to which they cancel is not *a priori* obvious.

#### C. Comparison with experiment

The open circles of Fig. 1 represent the 4f binding energies (relative to  $\epsilon_F$ ) measured in the room-temperature x-ray photoemission work<sup>8</sup> of Baer.  $\Delta_-$  results in which the 4f final state is the Hund's-rule ground multiplet are given by the lowest line of filled circles [labeled  $\Delta_-(1)$ ] in the figure. The

multiplet.<sup>7</sup> From this initial state several  $4f^{n-1}$  multiplet levels may be reached<sup>8</sup> after photoemission; one of these is the Hund's-rule ground multiplet of the final  $4f^{n-1}$  configuration. We will concentrate on the excitation energy for this final state in what follows. Our estimate of  $\Delta_-$  now separates naturally into four components; rewriting Eq. (2) we have

present results agree somewhat better<sup>9</sup> with experiment than do the results of I, the largest departure of theory from experiment being 1 eV for Ce and Yb. The over-all correspondence remains strikingly good.

Figure 1 also displays  $\epsilon_F - \epsilon_{4f_{7/2}}$ , the  $4f_{7/2}$  one-electron energy calculated for the metal and measured relative to the Fermi level.  $\epsilon_{4f_{7/2}}$  is smaller in magnitude than  $\epsilon_{4f_{5/2}}$ ; the difference between the two, which stems principally from the spin-orbit interaction, increases monotonically from 0.3 eV for Ce to 1.8 eV for Lu. These one-electron energies, which are evaluated in our band calculations, have been corrected to correspond to the Hund's-rule 4f state by the addition of  $(2/n)\delta E$ , where  $\delta E$  is the correction to the total energy of the initial state resulting from placing the 4f electrons into the Hund's-rule multiplet and  $n$  is the number of 4f electrons in the initial state. As was found<sup>10</sup> in I, the 4f one-electron energies grossly overestimate the observed 4f binding energies while the multielectron  $\Delta_-$  reproduce experiment extraordinarily well.

#### D. Final states of higher binding energy

Photoejection of an electron from the  $4f^n$  Hund's-rule multiplet will in general leave the  $f$  shell in

TABLE I. Components of  $\Delta_-$  (both initial and final 4f states are Hund's rule ground levels). See Eqs. (3) and (4) for definition of these terms; all energies in eV.

Element	$\xi$	$\delta E(\text{atom})$	$\delta E(\text{Hund})$	$\delta E(\text{atom} \rightarrow \text{band})$	$\Delta_-$
Ce	0.9	2.6	0.2	-1.8	1.9
Pr	0.9	3.3	1.3	-1.8	3.8
Nd	0.9	3.9	2.0	-1.7	5.1
Sm	1.6	4.9	0.8	-1.8	5.5
Eu	1.8	-0.4	2.3	-1.7	1.9
Gd	1.8	5.6	2.7	-1.8	8.3
Tb	3.7	5.9	-4.3	-2.0	3.3
Dy	3.2	6.2	-2.7	-2.0	4.7
Ho	2.9	6.3	-1.7	-2.0	5.5
Er	3.3	6.5	-2.4	-2.0	5.4
Tm	3.9	6.6	-3.2	-1.9	5.4
Yb	3.6	0.2	-0.7	-2.0	1.1
Lu	3.6	6.7	-0.8	-2.0	7.5

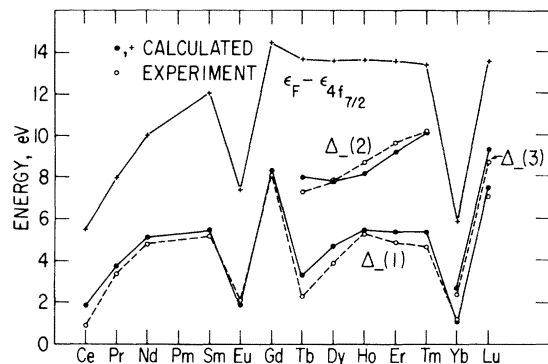


FIG. 1. Theoretical and experimental values for 4*f* photoexcitation energies in the rare-earth metals. The crosses are the one-electron predictions  $\epsilon_F - \epsilon_{4f7/2}$ ; the lower set of filled circles [ $\Delta_-(1)$ ] represents  $\Delta_-$  calculations in which the 4*f* final state is the Hund's-rule ground level; for Tb through Tm the upper filled circles [ $\Delta_-(2)$ ] are predictions for specific majority spin excitations, while for Yb and Lu the upper filled circles [ $\Delta_-(3)$ ] correspond to spin-orbit-split final states. Open circles are the experimental binding energies relative to  $\epsilon_F$ .

any of a number of the multiplets belonging to the  $4f^{n-1}$  configuration; one of these is the  $4f^{n-1}$  ground multiplet in terms of which  $\Delta_-$  was calculated above. The relative intensities of the lines corresponding to the various possible final states reflect<sup>8</sup> the coefficients of fractional parentage, i. e., the coefficients appearing in the expansion of the  $4f^n$  state in terms of products of  $4f^{n-1}$  states and a single  $4f$  orbital. These coefficients, which have been calculated<sup>8</sup> by Cox, together with the level ordering given by multiplet theory, permit consistent, unambiguous identification of the observed structures.

For Tb through Tm most of the peaks appearing at binding energies higher than that for the Hund's rule final 4*f* state arise from the excitation of a majority spin 4*f* electron from the over-half-filled 4*f* shell. In I we considered the states of spin  $S - 1$ , where  $S$  is the spin of the  $4f^{n-1}$  Hund's-rule ground state, and maximum possible  $L$ . For the metals from Tb to Tm these states are  $^6I$ ,  $^5L$ ,  $^4M$ ,  $^3M$ , and  $^2L$ , respectively. We scale the *f*-shell electrostatic integrals from our final state atomic calculations by a factor of 0.8 to roughly account for correlation effects. Use of these scaled integrals in the multiplet theory expressions<sup>11</sup> for the splitting between the above states and the appropriate Hund's-rule final ground-state levels produces the upper set of filled circles [labeled  $\Delta_-(2)$ ] for Tb through Tm in Fig. 1. Agreement with the data is gratifying. Multiplet theory, in combination with Slater integrals scaled by an over-all factor of about 0.8,

provides reasonable quantitative prediction of the energy splittings between the various final states. The calculated position of the peaks relative to  $\epsilon_F$ , of course, depends on the  $\Delta_-$  estimate for some specific final state, such as the ground state chosen here.

In the case of Yb and Lu, both of whose 4*f* shells are filled in the initial state, two 4*f* structures are observed. These correspond to the spin-orbit split  $^2F_{5/2}$  and  $^2F_{7/2}$  final states, the only ones possible. The separation of the higher-lying  $^2F_{5/2}$  multiplet from the  $^2F_{7/2}$  is given, to good approximation, by the difference  $\epsilon_{4f7/2} - \epsilon_{4f5/2}$ , which we obtain from our calculations for the  $4f^{13}$  final-state configurations. The upper theoretical points [ $\Delta_-(3)$ ] for Yb and Lu in Fig. 1 are determined in this way.  $\epsilon_{4f7/2} - \epsilon_{4f5/2}$  is in excellent accord with the splittings observed.

### III. ZERO SCREENING LIMIT

Electrically neutral atomic sites were assumed for the final states after photoemission in the preceding section. In this section we explore the impact of this approximation by performing calculations in which the atomic cell, after 4*f* photoejection, is constrained to have unit positive charge. There are two important contributions causing the resulting binding energies,  $\Delta_-(ion)$ , to differ from the  $\Delta_-$  of Sec. II. First, there is a change in the correlation energy contribution. Second, there is an energy change due to the absence of the screening charge; this will be estimated with band calculations similar to those of the preceding section and by computationally simpler free-atom estimates, and the results compared.

#### A. Correlation effects

We exploit free-atom and free-ion spectral data and ionization potentials to find the correlation energy difference  $\xi(ion)$  for the  $f^n d^{m-1} s \rightarrow f^{n-1} d^{m-1} s$  transition corresponding to  $\Delta_-(ion)$ . The measured<sup>12</sup> ionization potential is the splitting between the free-atom and free-ion ground states, and spectroscopic data for the free atom<sup>13</sup> and free ion<sup>14</sup> provide the splittings between the ground states of the  $f^n d^{m-1} s$  and  $f^{n-1} d^{m-1} s$  configurations, which are of interest to us here, and those entering the ionization potential. For example, the ionization potential<sup>12</sup> for neodymium is the ground state energy difference for the  $f^4 s^2 \rightarrow f^4 s$  transition; spectral data<sup>13,14</sup> furnish the splittings for the  $f^4 s^2 - f^3 d^2 s$  and  $f^4 s - f^2 d^2 s$  transitions, so that we can find the  $f^3 d^2 s - f^2 d^2 s$  ground-state energy difference. Coupling this information with our calculations for the  $f^n d^{m-1} s$  and  $f^{n-1} d^{m-1} s$  configurations we obtain  $\xi(ion)$ :

TABLE II. The correlation energy difference  $\xi(\text{ion})$  and screening energy estimates  $\Delta_S$  (atomic) and  $\Delta_S$  (band). See Eqs. (6), (9), and (10) for definition of these terms; all energies in eV.

Element	$\xi(\text{ion})$	$\Delta_S(\text{atomic})$	$\Delta_S(\text{band})$
Ce	1.9	5.0	3.9
Pr	1.6	5.0	4.1
Nd	1.9	4.9	4.2
Sm	2.8	4.8	4.3
Eu	2.6	3.8	4.5
Gd	2.7	4.6	4.6
Tb	4.9	4.6	4.7
Dy	4.6	4.5	4.8
Ho	4.2	4.4	4.8
Er	4.8	4.3	4.8
Tm	5.4	4.2	4.8
Yb	4.3	3.2	4.4
Lu	4.3	4.0	4.9

$$\begin{aligned}\xi(\text{ion}) &\equiv E_{\text{corr}}(f^{n-1} d^{m-1} s) - E_{\text{corr}}(f^n d^{m-1} s) \\ &= [E(f^{n-1} d^{m-1} s) - E(f^n d^{m-1} s)]_{\text{expt}} \\ &\quad - [E_{\text{band}}^{\text{RHF}}(f^{n-1} d^{m-1} s) - E_{\text{band}}^{\text{RHF}}(f^n d^{m-1} s)].\end{aligned}\quad (6)$$

The resulting values are listed in Table II; the spectral information<sup>13,14</sup> is uncertain for many of the states involved, but it suffices for our purposes here. Comparing  $\xi(\text{ion})$  with  $\xi$  of Table I we see that

$$\begin{aligned}\Delta_-(\text{ion}) &= \xi(\text{ion}) + [E_{(LS\text{ av})}^{\text{RHF}}(f^{n-1} d^{m-1} s) - E_{(LS\text{ av})}^{\text{RHF}}(f^n d^{m-1} s)] + [E(f^{n-1}) - E(f^n)]_{4f\text{ Hund's rule correction}} \\ &\quad + \{ [E_{\text{band}}^{\text{RHF}}(f^{n-1}(ds)^m) - E_{(LS\text{ av})}^{\text{RHF}}(f^{n-1} d^{m-1} s)] - [E_{\text{band}}^{\text{RHF}}(f^n(ds)^m) - E_{(LS\text{ av})}^{\text{RHF}}(f^n d^{m-1} s)] \} \\ &= \xi(\text{ion}) + \delta E(\text{free}) + \delta E(\text{Hund}) + \delta E(\text{free} \rightarrow \text{band}).\end{aligned}\quad (8)$$

Figure 2 compares  $\Delta_-(\text{ion})$  with  $\Delta_-$ . Screening<sup>15</sup> reduces the 4f binding energy by 4–6 eV. On this scale, the close agreement of  $\Delta_-$  with experiment suggests that the experimental situation corresponds closely to the complete screening limit.

### C. Alternate screening energy estimates

Noting that the  $\delta E(\text{Hund})$  components of Eqs. (4) and (8) agree to within 0.1 eV, we may write

$$\begin{aligned}\Delta_-(\text{ion}) - \Delta_- &\approx \xi(\text{ion}) - \xi \\ &\quad + [E_{\text{band}}^{\text{RHF}}(f^{n-1}(ds)^m) - E_{\text{band}}^{\text{RHF}}(f^{n-1}(ds)^{m+1})] \\ &\equiv \xi(\text{ion}) - \xi + \Delta_S(\text{band}),\end{aligned}\quad (9)$$

where  $\Delta_S(\text{band})$  is a RHF band estimate of the screening energy associated with the presence of an extra conduction electron. A computationally simpler scheme, which we have used<sup>16</sup> in other problems, is to calculate instead

$$\Delta_S(\text{atomic}) \equiv E_{(LS\text{ av})}^{\text{RHF}}(f^{n-1} d^{m-1} s) - E_{(LS\text{ av})}^{\text{RHF}}(f^{n-1} d^m s).\quad (10)$$

$$0.7 \text{ eV} \leq [\xi(\text{ion}) - \xi] \leq 1.5 \text{ eV}.\quad (7)$$

$\xi(\text{ion}) - \xi$  is the correlation energy associated with the extra 5d electron which is present in the neutral (screened) free-atom final state and not in the ionized (unscreened) final state.  $\xi(\text{ion})$  thus provides a measure of “bare” correlation associated with 4f electron excitation.

### B. Self-consistent band calculations

Our first approximation for  $\Delta_-(\text{ion})$  consists of implementing the procedure of Sec. II but using instead RHF calculations for the  $f^{n-1} d^{m-1} s$  free ion configuration as the input for the final-state total energy calculation. That is, we perform an RHF calculation for the  $f^{n-1} d^{m-1} s$  free ion, construct renormalized-atom crystal potentials, and carry out self-consistent band calculations, during the course of which the normalization of the wave functions to the Wigner-Seitz sphere insures that the final state cell has a charge of  $+1|e|$ , whereas for the computations described in Sec. II the cell was electrically neutral in the final state. The  $\bar{q}=0$  component of the full crystal potential, i. e., the potential arising from the charge of the other atomic cells, is *not* included in the total energy expression for the cell. Again, multiplet theory is used to correct the average of *LS* configuration energies and, in analogy with Eq. (4), we calculate

This is the free-atom screening energy associated with delivering a 5d screening electron to the final state atom.  $\Delta_S(\text{band})$  and  $\Delta_S(\text{atomic})$  are compared in Table II. Experience with 3d and 4d transition metals suggests that free-atom calculations significantly overestimate the screening energy for the metal; this is apparently not the case for the excitations studied here.

### ACKNOWLEDGMENT

One of us (JFH) is grateful to Brookhaven National Laboratory and the Laboratory of Atomic and Solid State Physics for the cordial hospitality extended to him.

### APPENDIX: GROUND-STATE ENERGY CORRECTIONS

The RHF computations described in this paper are performed within Lindgren’s average of *LS* configuration scheme, which averages over the  $L$ ,  $S$ ,  $M_L$ , and  $M_S$  quantum numbers of the open shells. In evaluating the correlation energy differences

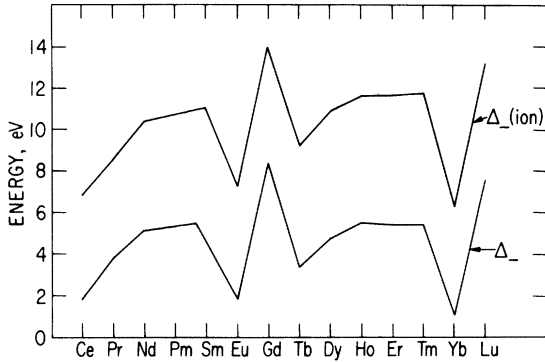


FIG. 2. Comparison of  $\Delta_-$  [ $\Delta_-(1)$  of Fig. 1] and  $\Delta_-(\text{ion})$ ; all  $4f$  final states are the Hund's rule ground multiplets. The difference between the two curves provides a measure of the energy associated with screening of the  $4f$  hole in the rare-earth metals.

and  $4f$  excitation energies, however, we require the total energies of the appropriate ground states. The necessary corrections are found by application of nonrelativistic (NR) Condon-Slater-Racah

$$\begin{aligned}
 E_{\text{tot}}(LS \text{ av}) - E_{\text{tot}}(gnd) = & -\frac{1}{21} F^2(4f, 5d) - \frac{4}{231} F^4(4f, 5d) + \frac{24}{35} G^1(4f, 5d) + \frac{46}{315} G^3(4f, 5d) - \frac{475}{7623} G^5(4f, 5d) \\
 & + \frac{53}{585} F^2(4f, 4f) + \frac{155}{4719} F^4(4f, 4f) - \frac{2975}{184041} F^6(4f, 4f) + \frac{58}{441} F^2(5d, 5d) - \frac{5}{441} F^4(5d, 5d) \\
 & + \frac{1}{5} G^2(5d, 6s) + \frac{1}{7} G^3(4f, 6s). \quad (\text{A1})
 \end{aligned}$$

For  $F^2(4f, 5d)$  we use the following multiplicity-weighted average:

$$\begin{aligned}
 F^2(4f, 5d) = & \frac{6}{14} \left[ \frac{4}{10} F^2(4f_{5/2}, 5d_{3/2}) \right. \\
 & + \frac{8}{10} F^2(4f_{5/2}, 5d_{5/2}) \\
 & + \frac{8}{14} \left[ \frac{4}{10} F^2(4f_{7/2}, 5d_{3/2}) \right. \\
 & \left. \left. + \frac{6}{10} F^2(4f_{7/2}, 5d_{5/2}) \right] \right];
 \end{aligned}$$

the RHF integrals are all  $2.5 \pm 0.1$  eV. The other integrals entering (A1) are similarly obtained, and we find

$$E_{\text{tot}}(LS \text{ av}) - E_{\text{tot}}(gnd) = 2.9 \text{ eV.}$$

The greatest disparity among RHF integrals corresponding to the same NR quantity occurs for the  $F^2(4fj, 4fj')$  of the heaviest elements; the largest of these integrals is  $17.0 \pm 0.3$  eV. Since differences of expressions such as (A1) appear in  $\xi$  and  $\xi(\text{ion})$ , the simplifications made here are entirely adequate for our purposes.  $\delta E(\text{Hund})$ , the  $4f$  ground-state correction [Eqs. (3) and (5)], involves differences between quantities such as

multiplet theory<sup>17</sup> with the use of the electrostatic integrals from the RHF calculations. Justification for employing the NR expressions lies in the fact that the RHF integrals  $R^k(nlj, n'l'j')$ , calculated in the average of  $LS$  configuration scheme for the  $4f$ ,  $5d$ , and  $6s$  electrons of interest here, are not very dependent on  $j$  and  $j'$ . If this independence were exact, then the relativistically correct multiplet expressions, whatever they are, would reduce to their NR analogs because the Dirac-Fock equations reduce to the HF equations when the speed of light is infinite. We circumvent the complications of  $j$ - $j$  coupling by averaging the  $R^k(nlj, n'l'j')$  over the values of  $j$  and  $j'$  to obtain an effective  $R^k(nl, n'l')$  which we then use in the NR multiplet equations. In addition, the RHF one-electron eigenvalues permit us to correct the total energies for spin-orbit effects.

We take the  $4f^2 5d^2 6s$  configuration ( ${}^6L_{11/2}$  ground state) of praseodymium as an example to detail these procedures. The difference between the average of  $LS$  configuration and ground-state total energies in the NR limit is

the sum of the sixth, seventh, and eighth terms on the right-hand side of Eq. (A1).

The spin-orbit correction to the total energy is found by calculating the expectation value of  $\lambda \vec{L} \cdot \vec{S}$  for the open shells, where  $\lambda$  is given by<sup>18</sup>

$$\lambda = \pm \zeta / 2s.$$

The plus sign is for less-than-half-filled shells and the minus sign for more-than-half-filled shells.  $\zeta$  is obtained from the RHF one-electron eigenvalues:

$$\begin{aligned}
 \zeta_{5d} &= \frac{2}{5} (\epsilon_{5d_{5/2}} - \epsilon_{5d_{3/2}}), \\
 \zeta_{4f} &= \frac{2}{7} (\epsilon_{4f_{7/2}} - \epsilon_{4f_{5/2}}).
 \end{aligned}$$

In the Pr example, the spin-orbit correction for the total ground-state energy is

$$\begin{aligned}
 \Delta E(\text{spin-orbit}) &= -\frac{6}{7} (\epsilon_{4f_{7/2}} - \epsilon_{4f_{5/2}}) \\
 &\quad - \frac{4}{5} (\epsilon_{5d_{5/2}} - \epsilon_{5d_{3/2}}) \\
 &= -0.4 \text{ eV.}
 \end{aligned}$$

In Table I the  $4f$  shell spin-orbit correction is included in  $\delta E(\text{Hund})$ .

\*Work supported by NRC-NBS Postdoctoral Research Associateship.

†Work supported in part by the NSF through Grant No.

DMR 74-23494.

†Part of work done while guest of Brookhaven National Laboratory.

<sup>8</sup>Work supported by the U. S. Energy Research and Development Administration.

<sup>1</sup>J. F. Herbst, D. N. Lowy, and R. E. Watson, *Phys. Rev. B* 6, 1913 (1972).

<sup>2</sup>R. E. Watson, H. Ehrenreich, and L. Hodges, *Phys. Rev. Lett.* 24, 829 (1970); L. Hodges, R. E. Watson, and H. Ehrenreich, *Phys. Rev. B* 5, 3953 (1972).

<sup>3</sup>I. Lindgren and A. Rosén, *Case Studies At. Phys.* 4, 93 (1974).

<sup>4</sup>I. P. Grant, *Adv. Phys.* 19, 747 (1970).

<sup>5</sup>In this work,  $\epsilon_{\Gamma_1}$ , the conduction-band minimum, and  $\epsilon_{d_{\min}}$ , the  $d$ -band minimum, are found by imposing the zero derivative condition on the  $6s$  and  $5d_{3/2}$  wave functions, respectively; the  $d$ -band maximum  $\epsilon_{d_{\max}}$  is that energy for which the  $5d_{5/2}$  wave function is noded

<sup>6</sup>See note 11 of Ref. 1.

<sup>7</sup>J. H. Van Vleck, *Theory of Electric and Magnetic Susceptibilities* (Oxford U.P., Oxford, 1959).

<sup>8</sup>Y. Baer, *J. Electron. Spectrosc. Relat. Phenom.* 5, 611 (1974), and references therein.

<sup>9</sup>The  $\Delta_{\cdot}$  values of Fig. 1 differ by no more than 0.3 eV from our earlier nonrelativistic calculations (I) for Ce, Pr, Nd, Sm, Gd, Ho, and Tm; the Dy and Er values are about 0.5 eV less than those of I, while in the case of Tb the present result is 1.0 eV smaller. For Eu and Yb the  $\Delta_{\cdot}$  of Fig. 1 are roughly 0.6 eV larger than the estimates presented in I. The changes in our  $\Delta_{\cdot}$  estimates, therefore, are not severe (with the possible exception of Tb).

<sup>10</sup>Compared to the  $\epsilon_F - \epsilon_{4f}$  values given in I, the results of Fig. 1 are all somewhat smaller, the decrease ranging from 0.4 eV (Ce) to 2.4 eV (Tm) for the trivalent metals, and 1.5 eV and 3.7 eV for Eu and Yb, re-

spectively. This decrease is the result of two competing influences. The relativistic contraction of the  $s$  and  $p$  shells lying within the  $4f$  makes the screening of the nucleus more effective so that the relativistic free-atom  $4f$  eigenvalues are less negative than their non-relativistic counterpart; but the self-consistent band treatment employed here, which was not attempted in I, works to lower the  $4f$  one-electron energy. The former effect evidently dominates.

<sup>11</sup>C. W. Nielson and G. F. Koster, *Spectroscopic Coefficients for the  $p^n$ ,  $d^n$ , and  $f^n$  Configurations* (MIT, Cambridge, 1963).

<sup>12</sup>W. C. Martin, L. Hagan, J. Reader, and J. Sugar, *J. Phys. Chem. Ref. Data* 3, 771 (1974).

<sup>13</sup>L. Brewer, *J. Opt. Soc. Am.* 61, 1101 (1971).

<sup>14</sup>L. Brewer, *J. Opt. Soc. Am.* 61, 1666 (1971).

<sup>15</sup>Since our treatment of the final states begins with a complete RHF atomic calculation, relaxation of the free-atom and free ion orbitals in the presence of the  $4f$  hole (or  $4f$  hole plus  $5d$  screening electron) is implicitly included in the  $\Delta_{\cdot}$  and  $\Delta_{\cdot}$  (ion) estimates. Only if this intra-atomic screening is comparable for  $\Delta_{\cdot}$  and  $\Delta_{\cdot}$  (ion) can we strictly identify  $\Delta_{\cdot}$ (ion) -  $\Delta_{\cdot}$  with the extra-atomic screening energy often discussed in the recent literature.

<sup>16</sup>R. E. Watson, J. F. Herbst, and J. W. Wilkins (unpublished); R. E. Watson, M. L. Perlman, and J. F. Herbst (unpublished).

<sup>17</sup>J. C. Slater, *Quantum Theory of Atomic Structure* (McGraw-Hill, New York, 1960), Vols. I and II.

<sup>18</sup>M. Blume, A. J. Freeman, and R. E. Watson, *Phys. Rev.* 134, A320 (1964).